

where  $R^*$  is the binding energy of excitons,  $\kappa$  is the dielectric constant, and  $m^*$  is the reduced mass of excitons. If we take  $m^* = 0.036m_0$  estimated from the cyclotron mass of electrons and holes at 88 T and  $\kappa = 100$ , we obtain  $\gamma = 2890$  at 88 T. The binding energy of excitons is then estimated to be 4.6 meV.<sup>18</sup> Thus it is worthwhile to investigate in more detail this interesting problem of the phase transition which might occur near the gapless state in very high magnetic fields.

<sup>(a)</sup>Present address: Central Research Laboratory, Hitachi Ltd., Kokubunji, Tokyo, Japan.

<sup>1</sup>M. P. Vecchi, J. R. Pereira, and M. S. Dresselhaus, Phys. Rev. B **14**, 298 (1976).

<sup>2</sup>G. A. Baraff, Phys. Rev. **137**, A842 (1965).

<sup>3</sup>N. B. Brandt, E. A. Svistova, and Yu. G. Kashirskii, Pis'ma Zh. Eksp. Teor. Fiz. **9**, 232 (1969) [JETP Lett. **9**, 136 (1969)].

<sup>4</sup>K. Hiruma, G. Kido, K. Kawauchi, and N. Miura, Solid State Commun. **33**, 257 (1980).

<sup>5</sup>N. B. Brandt and E. A. Svistova, J. Low Temp. Phys. **2**, 1 (1970).

<sup>6</sup>N. F. Mott, Philos. Mag. **6**, 287 (1961).

<sup>7</sup>T. Sakai, N. Goto, and M. Mase, J. Phys. Soc. Jpn. **35**, 1064 (1973).

<sup>8</sup>D. Yoshioka, J. Phys. Soc. Jpn. **45**, 1165 (1978).

<sup>9</sup>S. Nakajima and D. Yoshioka, J. Phys. Soc. Jpn. **40**, 328 (1976).

<sup>10</sup>N. Miura, G. Kido, M. Akihiro, and S. Chikazumi, J. Magn. Magn. Mater. **11**, 275 (1979).

<sup>11</sup>G. Kido, N. Miura, H. Katayama, and S. Chikazumi, J. Phys. E **14**, 349 (1981).

<sup>12</sup>K. Hiruma and Miura, to be published.

<sup>13</sup>S. Takano and H. Kawamura, J. Phys. Soc. Jpn. **28**, 348 (1970).

<sup>14</sup>K. Hiruma, G. Kido, and N. Miura, Solid State Commun. **31**, 1019 (1979).

<sup>15</sup>K. Hiruma and N. Miura, to be published.

<sup>16</sup>G. E. Smith, G. A. Baraff, and J. M. Rowell, Phys. Rev. **135**, A1118 (1964).

<sup>17</sup>K. Hiruma, G. Kido, and N. Miura, Solid State Commun. **38**, 859 (1981).

<sup>18</sup>Y. Yafet, R. W. Keys, and E. N. Adams, J. Phys. Chem. Solids **1**, 137 (1956).

## Anisotropic Superconducting and Magnetic Properties of a Single Crystal of ErRh<sub>4</sub>B<sub>4</sub>

G. W. Crabtree, F. Behroozi,<sup>(a)</sup> S. A. Campbell,<sup>(b)</sup> and D. G. Hinks

*Solid State Science Division, Argonne National Laboratory, Argonne, Illinois 60439*

(Received 9 August 1982)

The magnetic response of a single crystal of the tetragonal compound ErRh<sub>4</sub>B<sub>4</sub> in the  $\bar{c}$  (hard) and  $\bar{a}$  (easy) directions is presented. Extreme anisotropy is found in the magnetic and superconducting behavior, allowing a natural separation of the bare superconducting properties from those affected by magnetism. Below  $T_{c2}$  the data reconcile the discrepancy between the ferromagnetic moment per erbium atom measured by neutron scattering and by Mössbauer effect.

PACS numbers: 74.70.Rv, 75.30.Cr

Reentrant superconductivity found in the stoichiometric compounds ErRh<sub>4</sub>B<sub>4</sub> and HoMo<sub>6</sub>S<sub>8</sub> provides a unique opportunity to study the interaction of superconductivity and ferromagnetism.<sup>1,2</sup> As the temperature is lowered, ErRh<sub>4</sub>B<sub>4</sub> transforms through four distinct phases: paramagnetic for  $T > T_{c1} = 8.6$  K, superconducting for  $T_{c1} \geq T \geq 1.2$  K, coexistence for  $1.2 \text{ K} \geq T > T_{c2} = 0.7$  K, and normal ferromagnetic for  $T < T_{c2}$ . Considerable work on polycrystalline specimens has yielded much information on the thermal,<sup>3</sup> paramagnetic,<sup>1,4</sup> superconducting,<sup>5-8</sup> and ferromagnetic behavior<sup>9,10</sup> of ErRh<sub>4</sub>B<sub>4</sub>. Recently, neutron scattering from a single crystal of ErRh<sub>4</sub>B<sub>4</sub> has provided detailed information on the coexistence

phase.<sup>11</sup> However, none of this work has examined the important role that anisotropy plays in determining the superconducting and magnetic properties of the various phases.

In this paper we report on the magnetic response of a single crystal of the tetragonal compound ErRh<sub>4</sub>B<sub>4</sub> in the  $\bar{c}$ (hard) and  $\bar{a}$ (easy) directions. Both ac susceptibility and dynamic dc susceptibility and magnetization data were obtained in fields between 0 and 20 kOe and temperatures between 0.4 and 15 K. The ac measurements were obtained with a mutual inductance bridge operating at 79 Hz with an excitation field of 1 Oe. The dc measurements utilized the net signal from a balanced pair of opposing coils, one containing

the sample, as the external field was varied. A more complete description of the ac and dc techniques is given elsewhere.<sup>8,12</sup> The single crystal was grown by solidification of a nonstoichiometric Er-Rh-B melt. The ingot contained a bicrystal, which was cut along its grain boundary to yield two single crystals. The larger of these was used for neutron-scattering experiments,<sup>11</sup> while part of the smaller crystal was used to form a sphere of diameter  $\approx 1$  mm with less than 5% variation in radius for the work presented here. With this geometry, the internal field  $H_i$  is related to the applied field  $H_a$  by  $H_i = H_a - 4\pi nM$  for all crystallographic directions. In this expression  $M$  is the magnetization and  $n$  is the demagnetizing factor which equals  $\frac{1}{3}$  for a sphere.

Typical dc magnetization curves for the  $\bar{a}$  and  $\bar{c}$  directions are shown in Fig. 1. Unlike the data for polycrystalline specimens<sup>5,7,8</sup> the overall hysteresis due to flux pinning and flux trapping is relatively mild. At low fields there is a linear

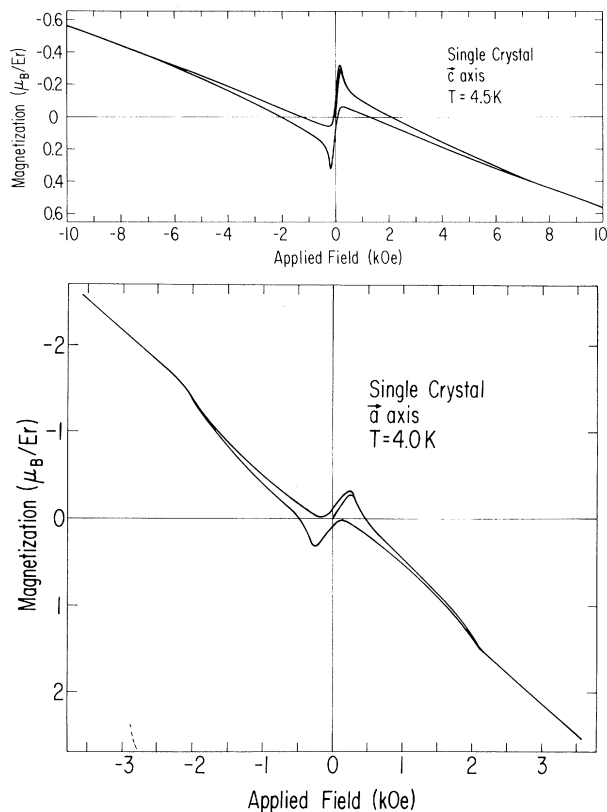


FIG. 1. Magnetization curves for the  $\bar{c}$  and  $\bar{a}$  directions of  $\text{ErRh}_4\text{B}_4$  in the superconducting phase, as functions of the applied field. Note the compression of the horizontal scale and expansion of the vertical scale for the  $\bar{c}$  direction relative to the  $\bar{a}$  direction.

Meissner region where all magnetic flux is excluded from the sample. Flux begins to enter the specimen at  $H_{c1}$  causing the slope of the magnetization curve to change sign as the mixed vortex phase is established. In this field region the Er moments inside the vortex cores are polarized and eventually cause the net magnetization to become paramagnetic as the applied field is increased. At  $H_{c2}$ , superconductivity is destroyed and the specimen enters the paramagnetic phase. For applied fields up to 20 kOe, the magnetization in the  $\bar{c}$  direction remains nearly linear while in the  $\bar{a}$  direction it shows considerable curvature as the moments begin to saturate.

In the paramagnetic region when  $H > H_{c2}$ , the slope and magnitude of the magnetization curve are far smaller along  $\bar{c}$  than along  $\bar{a}$ , implying a much smaller magnetic susceptibility in the  $\bar{c}$  direction. (In Fig. 1, the normal-state susceptibilities for the two directions differ by more than a factor of 10.) Thus, apart from a small paramagnetic component for  $H > H_{c1}$ , the magnetization in the  $\bar{c}$  direction is very similar to that of an ordinary type-II superconductor. In sharp contrast, the  $\bar{a}$ -direction magnetization displays unusual features which are not found in ordinary superconductors. In particular, the downward curvature in the magnetization extending from about 1 kOe to  $H_{c2}$  is opposite to that expected for bare superconducting behavior, and is absent in the  $\bar{c}$ -direction data. It is observed in the  $\bar{a}$ -direction magnetization curves for all temperatures between  $T_{c1}$  and about 1.4 K, becoming progressively more prominent as the temperature is lowered. Below 3 K, the downward curvature culminates in a discontinuous drop of the magnetization at  $H_{c2}$ , implying a first-order phase transition into the normal state. This is different from type-I superconducting behavior since, for the temperature range 3–1.4 K,  $H_{c2}$  is considerably larger than  $H_{c1}$  as illustrated in Fig. 2 below. A first-order phase transition at  $H_{c2}$  is unusual in superconductivity, and implies an attractive interaction between the vortex lines.<sup>13,14</sup>

From the magnetization curves we have determined the superconducting critical fields for both directions as functions of temperature (Fig. 2). Because of rounding in the magnetization near  $H_{c1}$ , there is some uncertainty as to where the Meissner region ends. We have taken  $H_{c1}$  to be the field at which the magnetization first deviates from linearity. However, even this method may well overestimate the value of  $H_{c1}$  since flux entry into the specimen is inhibited by pinning and

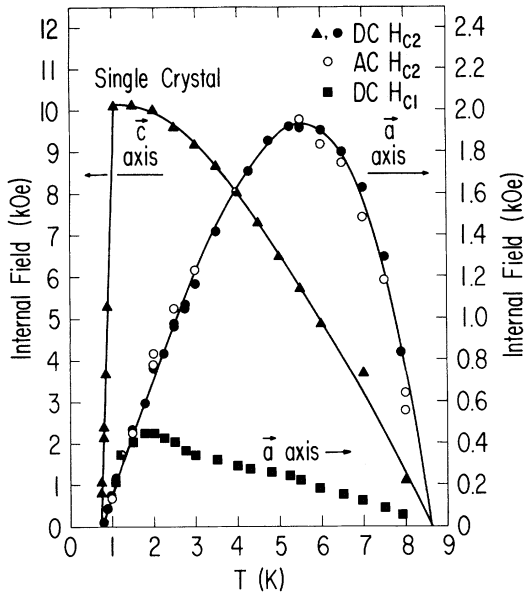


FIG. 2. The upper critical field  $H_{c2}$  for the  $\bar{c}$  and  $\bar{a}$  directions of  $\text{ErRh}_4\text{B}_4$  as a function of temperature. The right-hand vertical scale is for the  $\bar{a}$  direction and has been expanded by a factor of 5. For clarity, the lower critical field  $H_{c1}$  is shown for the  $\bar{a}$  direction only. The magnitude and temperature dependence of  $H_{c1}$  for the  $\bar{c}$  direction are similar to those for the  $\bar{a}$  direction.

surface barriers. The upper critical field  $H_{c2}$  is identified by the break in the slope of the magnetization curve when the sample enters the paramagnetic state. In the  $\bar{c}$  direction this change in the slope at  $H_{c2}$  is less obvious than in the  $\bar{a}$  direction, but can be identified in the dc susceptibility signal. The upper and lower critical fields measured by ac susceptibility confirm the dc results.

The critical field in the  $\bar{c}$  direction rises nearly parabolically as the temperature is lowered from  $T_{c1}$  to about 1.2 K as in ordinary type-II superconductors. The absence of any obvious magnetic effects is consistent with the low value of the induced moment along  $\bar{c}$ . However, the critical field falls sharply at about 1.2 K where neutron measurements show the first appearance of an ordered moment signifying the onset of the coexistence phase.<sup>11</sup> A similar drop also occurs in  $H_{c1}$  at  $T \approx 1.2$  K.

In the  $\bar{a}$  direction  $H_{c2}$  behaves quite differently from ordinary superconductors, displaying a peak at 5.5 K. This peak and the much smaller upper critical field can be understood qualitatively by a simple free-energy argument.<sup>8</sup> The magnetic contribution to the Gibbs free energy of the

normal state is given by  $-\int_0^H M dH \approx -\frac{1}{2}\chi H^2$  in the presence of a field. Since  $\chi$  is small along  $\bar{c}$  but very large along  $\bar{a}$ , the normal state is energetically favorable with respect to the superconducting state at a much smaller field along the  $\bar{a}$  direction. The peak in  $H_{c2}$  can be attributed to the dramatic increase in  $\chi$  as the temperature is lowered toward 1.2 K which makes the normal state favorable at successively lower fields.

In the vicinity of 1.4 K,  $H_{c2}$  joins  $H_{c1}$ , indicating a transition to type-I behavior, similar to that reported for polycrystalline specimens.<sup>7,8</sup> Since there is some uncertainty in values of  $H_{c1}$  from the magnetization curves, it is impossible to determine from our data whether  $H_{c1}$  meets  $H_{c2}$  at the onset of the coexistence phase or slightly above it.

The anisotropy in  $H_{c2}$  for the two directions explains some puzzling features of the polycrystalline results.<sup>4-8</sup> For example, typical magnetization curves for polycrystalline samples show a large hysteresis loop followed by a less prominent hysteretic tail.<sup>8</sup> The main loop is due to the  $\bar{a}$ -direction behavior while the long tail reflects the much larger  $H_{c2}$  associated with the  $\bar{c}$  direction. The large discrepancy<sup>5</sup> in the resistive and magnetic measurements of  $H_{c2}$  in polycrystalline samples is also due to the large anisotropy in  $H_{c2}$ . The resistive method measures the large values of  $H_{c2}$  in the  $c$  direction while the magnetic method measures the much smaller values associated with the  $\bar{a}$  direction.

Figure 3 shows the induced moment as a function of the *internal* field for both directions. The  $\bar{c}$ -direction data imply that the spontaneous moment is confined to the basal plane, consistent with neutron-scattering measurements<sup>9-11</sup> which show that the moments are polarized along  $\bar{a}$ . Although at this temperature the crystal is in the ferromagnetic state, the  $\bar{c}$ -direction behavior is similar to that for a weak paramagnet with a small induced moment which increases linearly with the field.

The  $\bar{a}$ -direction data show ideal ferromagnetic behavior with the magnetization rising smoothly from a spontaneous value of  $(5.7 \pm 0.2) \mu_B/\text{Er}$  at zero internal field to a saturation value of  $(8.5 \pm 0.2) \mu_B/\text{Er}$  at 7 kOe internal field. The arrows in Fig. 3 indicate the value of the spontaneous moment where the magnetization curve begins to deviate from the vertical  $H_i = 0$  axis. Although this feature is difficult to see in Fig. 3, it is clearly evident in the raw data where the magnetization is recorded as a function of the applied

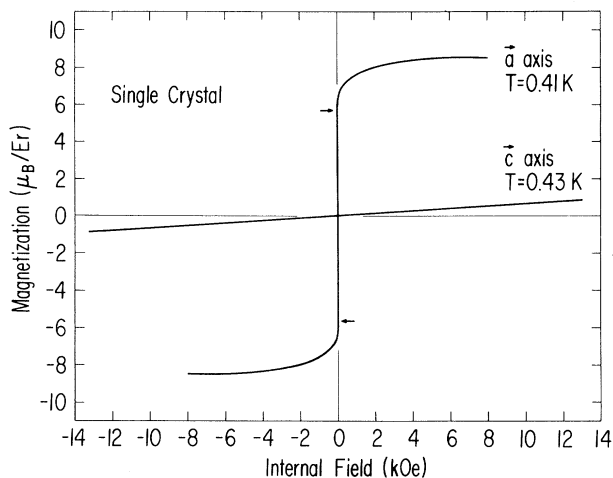


FIG. 3. Magnetization curves for the  $\bar{c}$  and  $\bar{a}$  directions of  $\text{ErRh}_4\text{B}_4$  in the ferromagnetic phase, as a function of the *internal* field. The arrows indicate the value of the spontaneous moment as discussed in the text.

field. The complete absence of hysteresis in the  $\bar{a}$ -direction data indicates that the magnetic domain boundaries move freely as the applied field is varied. The free movement of the domain boundaries is consistent with the mild hysteresis in the superconducting phase, and implies a low concentration of defects in the specimen which may serve as pinning centers.

The large magnetic anisotropy in  $\text{ErRh}_4\text{B}_4$  arises naturally in a crystal-field model developed by Dunlap and Niarchos<sup>15</sup> where a doublet composed of angular momentum states  $J_z = \pm \frac{3}{2}$  and  $\mp \frac{5}{2}$  lies 1.4 K above a doublet having states  $\pm \frac{1}{2}$  and  $\mp \frac{7}{2}$ . This model fits our magnetization data in the paramagnetic state and can be generalized to account for data on other ternary borides.

The  $\bar{a}$ -direction spontaneous and saturation moments are in excellent agreement with values measured by neutron scattering<sup>9</sup> ( $5.6 \mu_B/\text{Er}$ ) and Mössbauer effect<sup>16</sup> ( $8.3 \mu_B/\text{Er}$ ). Our measurement thus reconciles this basic discrepancy, and suggests that a neutron measurement of the saturation moment would agree with the Mössbauer result. However, the neutron measurement shows that the moment in zero field is constant<sup>9</sup> at  $5.6 \mu_B/\text{Er}$  for  $T < 0.4$  K, implying that the spontaneous moment never equals the saturation moment, even at  $T=0$ . The reason for this unusual behavior remains to be explained.

We are grateful for the assistance of L. N. Hall in carrying out this work. This work was supported by the U. S. Department of Energy.

<sup>(a)</sup>On leave from University of Wisconsin, Parkside, Kenosha, Wisc. 53141.

<sup>(b)</sup>Present address: Sperry Univac, P.O. Box 3524, St. Paul, Minn. 55165.

<sup>1</sup>W. A. Fertig, D. C. Johnston, L. E. DeLong, R. W. McCallum, M. B. Maple, and B. T. Matthias, Phys. Rev. Lett. **38**, 987 (1977).

<sup>2</sup>Ø. Fischer, A. Treyvaud, R. Chevrel, and M. Sergent, Solid State Commun. **17**, 21 (1975); J. W. Lynn, G. Shirane, W. Thomlinson, and R. N. Shelton, Phys. Rev. Lett. **46**, 368 (1981).

<sup>3</sup>L. D. Woolf, D. C. Johnston, H. B. MacKay, R. W. McCallum, and M. B. Maple, J. Low Temp. Phys. **35**, 651 (1979); H. B. MacKay, L. D. Woolf, M. B. Maple, and D. C. Johnston, Phys. Rev. Lett. **42**, 918 (1979).

<sup>4</sup>F. Behroozi, G. W. Crabtree, S. A. Campbell, M. Levy, D. R. Snider, D. C. Johnston, and B. T. Matthias, Solid State Commun. **39**, 1041 (1981).

<sup>5</sup>H. R. Ott, W. A. Fertig, D. C. Johnston, M. B. Maple, and B. T. Matthias, J. Low Temp. Phys. **33**, 159 (1978).

<sup>6</sup>F. Behroozi, M. Levy, D. C. Johnston, and B. T. Matthias, Solid State Commun. **38**, 515 (1981).

<sup>7</sup>H. Adrain, K. Muller, and G. Saemann-Ischenko, Phys. Rev. B **22**, 4424 (1980).

<sup>8</sup>F. Behroozi, G. W. Crabtree, S. A. Campbell, D. R. Snider, S. Schneider, and M. Levy, J. Low Temp. Phys. **49**, 73 (1982).

<sup>9</sup>D. E. Moncton, D. B. McWhan, J. Eckert, G. Shirane, and W. Thomlinson, Phys. Rev. Lett. **39**, 1164 (1977).

<sup>10</sup>D. E. Moncton, D. B. McWhan, P. H. Schmidt, G. Shirane, W. Thomlinson, M. B. Maple, H. B. MacKay, L. D. Woolf, Z. Fisk, and D. C. Johnston, Phys. Rev. Lett. **45**, 2060 (1980).

<sup>11</sup>S. K. Sinha, G. W. Crabtree, D. G. Hinks, and H. Mook, Phys. Rev. Lett. **48**, 950 (1982).

<sup>12</sup>S. A. Campbell, J. B. Ketterson, and G. W. Crabtree, to be published.

<sup>13</sup>M. Tachiki, H. Matsumoto, and H. Umezawa, Phys. Rev. B **20**, 1915 (1979).

<sup>14</sup>M. Tachiki, in Proceedings of the Fourth Conference on Superconductivity in *d*- and *f*-Band Metals, Karlsruhe, West Germany 20-30 June 1982 (to be published).

<sup>15</sup>B. D. Dunlap and D. Niarchos, to be published.

<sup>16</sup>G. K. Shenoy, B. D. Dunlap, F. Y. Fradin, S. K. Sinha, W. Potzel, F. Pröbst, and G. M. Kalvius, Phys. Rev. B **21**, 3886 (1980).